JOURNAL OF SOLID STATE CHEMISTRY 68, 94–105 (1987)

The Vibrational Spectra and Normal Coordinate Analyses of Cubic and Monoclinic SiP_2O_7

I. N. CHAKRABORTY AND R. A. CONDRATE, SR.

NYS College of Ceramics, Alfred University, Alfred, New York 14802

J. R. FERRARO

Chemistry Department, Loyola University, Chicago, Illinois 60626

AND C. F. CHENUIT

GTE, Towanda, Pennsylvania 18848

Received May 19, 1986; in revised form September 11, 1986

The infrared and Raman spectra of cubic and monoclinic SiP_2O_7 were measured and interpreted by normal coordinate analyses using a modified valence force field. Band assignments were made for the vibrational modes of these materials, including those that involved the SiO_6 units. The calculated force constants for the SiO_6 and the P_2O_7 units were consistent with those for SiO_4- and P_2O_7-containing materials as well as stishovite. The Si–O stretching force constants for the SiO_6 units were considerably lower than those for SiO_4 units. © 1987 Academic Press, Inc.

Introduction

Crystalline materials with equimolar amounts of SiO_2 and P_2O_5 are structurally unique because of the sixfold coordination for their silicon atoms. SiP_2O_7 exists in six polymorphic forms. X-ray diffraction data reveal that the silicon atoms in all these polymorphs are octahedrally coordinated by oxygen atoms, and all phosphorus atoms are tetrahedrally coordinated (*1, 2*). Similar coordination for silicon has been noted for one silica phase (stishovite) which is synthesized at high temperatures and pressures. In this paper, the infrared and Raman spectra of the cubic and one of the monoclinic ($P2_1/c$) SiP_2O_7 phases are analyzed by normal coordinate analysis (NCA) both to make band assignments for their vibrational modes and to obtain new structural information from their calculated force constants.

Experimental

The two investigated polymorphic forms of SiP_2O_7 (cubic ($Pa3$) and monoclinic ($P2_1/c$)) were synthesized by the procedures developed by Makart (*2*). They were prepared by mixing 99.999% pure silica and puratronic grade ammonium dihydrogen phosphate with a 3% excess of P_2O_5. This excess of P_2O_5 was added to account for anticipated volatilization during the reaction. The components were blended and ball-milled in acetone with an alumina

0022-4596/87 $3.00

grinding medium for 2 hr to achieve the appropriate particle intimacy. The milled slurry was filtered and dried before firing in a covered silica crucible at 650°C for about 2 hr. This material was ground, passed through a 200-mesh screen, and fired in a covered platinum crucible for 10 days at 630°C to obtain the monoclinic polymorph. The cubic polymorph was obtained by firing the mix at 1100°C for 40 hr. Temperatures were maintained within ±10°C.

The formation of the investigated SiP_2O_7 polymorphs was monitored with an automated powder diffractometer. The measured powder X-ray diffraction pattern for cubic SiP_2O_7 was compared with that reported in the literature (*3*). Due to the unavailability of a reported diffracton pattern for monoclinic ($P2_1/c$) SiP_2O_7, the observed pattern was compared with the calculated pattern. The latter pattern was computed with an available FORTRAN program (*4*), using relevant crystal data obtained by Bisert and Liebau (*5*). The calculated *d*-spacings are compred with the observed values in Table I. Differences in the relative intensities between the observed and calculated patterns can be attributed to preferred orientation effects. The X-ray diffraction patterns of the investigated samples showed no diffraction lines originating from impurity phases.

The infrared absorption spectra were measured in the 4000- to 300-cm^{-1} region with a double-beam grating spectrophotometer equipped with a purging device to maintain a moisture- and CO_2-free atmosphere in the instrument. These spectra were obtained using KBr pellets. The instrument was calibrated with a standard polystyrene sheet. The absorption bands were reproducible to ±2 cm^{-1}. A Fourier transform IR (FTIR) spectrophotometer measured their far-infrared spectra in the diffuse reflectance mode. Samples were diluted with polyethylene powder for these latter spectral measurements.

TABLE I

POWDER X-RAY DIFFRACTION DATA FOR MONOCLINIC ($P2_1/c$) SiP_2O_7

Calculated		Observed	
d (Å)	I/I_o	*d* (Å)	I/I_o
5.814	12	5.8221	25.81
4.798	3	4.8054	5.65
3.981	18	3.9795	14.72
3.789	24	3.7885	23.44
3.670	100	3.6772	100.00
3.370	26	3.3651	25.53
3.180	58	3.1811	37.38
3.094	14	3.0966	6.48
2.907	11	2.9072	7.09
2.668	8	2.6711	3.60
2.659	5	2.6596	2.01
2.589	41	2.5901	16.82
2.476	5	—	—
2.365	16	2.3699	3.88
2.325	7	2.3169	7.98
2.317	21	—	—
2.250	2	—	—
2.215	13	2.2152	3.29
2.191	5	—	—
2.178	13	2.1768	3.18
2.155	2	—	—
2.140	17	2.1398	4.61
2.122	2	—	—
2.089	14	—	—
2.057	24	2.0576	5.98
2.020	6	—	—

Plus 24 more calculated lines above 1.522 Å.

The Raman spectra were measured using a double-grating spectrometer with an argon ion laser as an excitation source. Scattered radiation was collected at 90° to the direction of the incident laser beam. The instrument was calibrated with distilled indene, and the bands were reproducible to ±1 cm^{-1}.

The NCA treatment of crystals was similar to that of molecules with the additional limitation that the motions of their atoms were constrained by Born–von Karman (BvK) boundary conditions (*6*, *7*). Details

of the computation method have been described elsewhere (*8*). For both cubic and monoclinic SiP_2O_7, the average difference between the assigned observed and calculated wavenumbers is below 3%. In a few cases where bands in certain infrared or Raman regions are close together (for example, at ca. 450 cm^{-1} in the Raman spectra), there might be some uncertainty in the present assignments for these bands. A future investigation using both isotopic substitution, including silicon isotopes, and polarizability measurements with large single crystals may be necessary to conclusively substantiate these assignments.

Results and Discussion

A. Structural Considerations for Cubic SiP_2O_7

Cubic SiP_2O_7 belongs to space group T_h^6 ($Pa3$) with the cell parameter a = 7.46 Å and four formula units per unit cell. The atomic arrangement for this material is illustrated in Fig. 1. Its Bravais unit cell consists of four SiO_6 octahedral and eight PO_4 tetrahedral units (*9*). The Si–O bond distances in the SiO_6 octahedral units are 1.835 Å. The PO_4 tetrahedral units possess three short phosphorus–oxygen bonds ($P–O_I$) with a bond length of 1.38 Å and a longer bond ($P–O_{II}$) with a bond length of 1.41 Å. The six oxygen atoms of the octahedral units are connected to different PO_4 tetrahedral units. Also, only three oxygen atoms (O_I-type) on the tetrahedral units are shared by different SiO_6 octahedral units. The other oxygen atom (O_{II}-type) is shared by another tetrahedral unit to form a $P–O_{II}–P$ bridge.

Only stretching and bending coordinates were considered for the NCA treatment of this structure. Seventy-four atoms were needed to define the set of internal coordi-

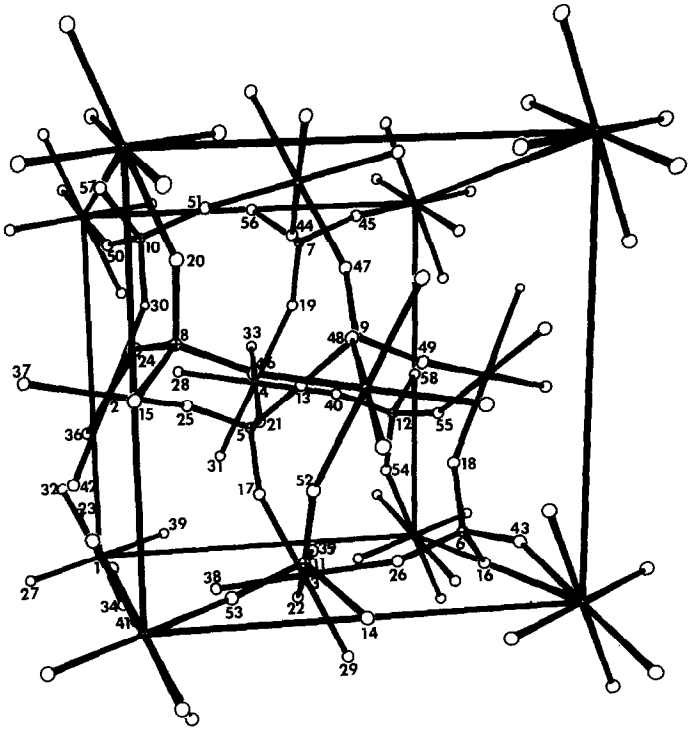

FIG. 1. Atomic arrangement in cubic SiP_2O_7.

nates of the unit cell on the basis of factor group and $k = 0$ selection rules. Atoms numbered from 1 to 58 are shown in Fig. 1. Translationally equivalent atoms in the lattice were considered to be nonequivalent atoms for defining the internal coordinates. The equivalency of these atoms was taken into consideration for the G-matrix calculation by incorporating the BvK correction. The fractional coordinates of all 74 atoms needed to define the internal coordinates and the corresponding translationally equivalent atoms in the cell are reported elsewhere (*10*). The internal coordinates were defined on the basis of the information obtained from the ORTEP program (*11*). The 188 symmetry coordinates needed to define the cubic unit cell uniquely are reported elsewhere (*10*).

The factor group analysis predicts the following selection rules for the cubic phase:

$$\underset{(R)}{4A_g} + \underset{(ia)}{6A_u} + \underset{(R)}{4E_g} + \underset{(ia)}{6E_u} + \underset{(R)}{12F_g} + \underset{(IR)}{17F_u}.$$

Only the vibrations with F_u-symmery are infrared active, and the vibrations with A_g-, E_g-, and F_g-symmetry are Raman active. The selection rule predicts 17 infrared-active and 20 Raman-active bands. No coincidences are expected on the basis of the mutual exclusion principle. A modified valence force field has been used for the calculation of the first-order wavenumbers. Three stretching force constants, f_{ra}, f_{rb} and f_{rc}, are associated with Si–O, P–O_I, and P–O_{II} stretching coordinates, respectively. Six bending force constants, f_{aa}, f_{ab}, f_{ac}, f_{ad}, f_{ae}, and f_{af}, are associated with O–Si–O (107.7°), O–Si–O (72.2°), O_I–P–O_I, O_I–P–O_{II}, Si–O_I–P, and P–O_{II}–P bending coordinates, respectively. In order to obtain a better fit between the observed and calculated wavenumbers, five stretching–stretching and stretching–bending interactions were also incorporated. The force constants, f_{rara}, f_{raaa}, f_{raab}, f_{rbrb}, and f_{rbac}, are associated with the (Si–O) (Si–O), (Si–O) (O–Si–O large angle), (Si–O) (O–Si–O small angle), (P–O) (P–O), and (P–O) (O–P–O) interactions, respectively. The interactions between all types of P–O stretching coordinates were approximated to be the same. A similar approximation was made for all interactions between P–O stretching and O–P–O bending coordinates.

B. Vibrational Spectral Analysis for Cubic SiP_2O_7

The infrared and Raman spectra for cubic SiP_2O_7 crystals are illustrated in Figs. 2 and

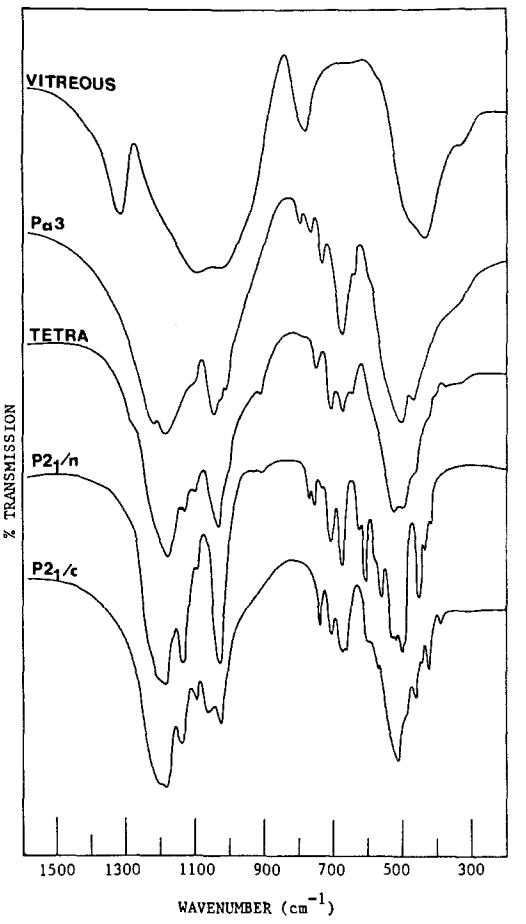

FIG. 2. The infrared spectra of various SiP_2O_7 polymorphs.

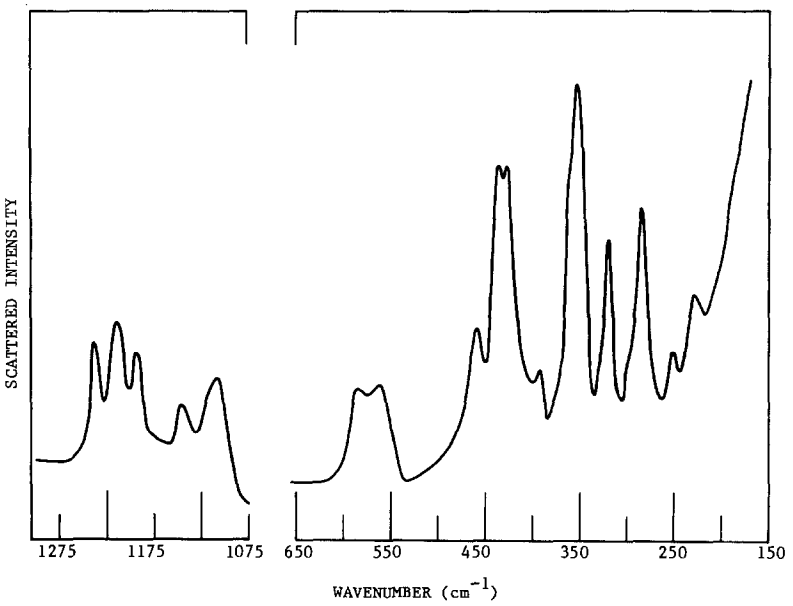

FIG. 3. The Raman spectrum of cubic SiP_2O_7.

3, respectively. The far-infrared spectrum of this crystal is illustrated in Fig. 4. Table II lists the observed and calculated wavenumbers along with major contributors for each mode of vibration. Each of the latter mentioned coordinates contributes more than 5% to the potential energy distribution of the particular mode. Some contributors for some of the bands may be neglected during the following text discussion because their contribution to the potential energy distributions for the modes may be at the lower end of the percentage scale. Due to overlapping of bands and weak intensities, a smaller number of bands are observed in the infrared and Raman spectra than are predicted by factor group analysis. One may also note the effect of stronger covalent bonding for the metal–oxygen (Si–O) bonds upon band locations for P–O stretching modes. In some cases, bands associated with $P–O_I$ bonds appear at lower wavenumbers than those for $P–O_{II}$ bonds because of coupling of the vibrational motions of the former bonds with those of $Si–O_I$ bonds linked to them.

According to factor group analysis, all of the infrared-active bands belong to F_u-symmetry. The strongest infrared bands at 1230 and 1195 cm^{-1} are assigned to primarily P–O stretching vibrations. Corresponding bands in Raman spectra appear at 1212 and 1192 cm^{-1}. The latter bands are assigned to modes with F_g- and E_g-symmetry species, respectively. The medium intensity shoulder at ca. 1100 cm^{-1}, the strong band 1052 cm^{-1}, and the weak band at 732 cm^{-1} in the infrared spectrum are also assigned primarily to P–O stretching vibrations. The Raman bands at 1143 and 1107 cm^{-1} are assigned to P–O stretching vibrations with F_g- and A_g-symmetry, respectively. The infrared band at 798 cm^{-1} is assigned to a Si–O stretching vibration of the SiO_6 octahedral units. As expected, the Si–O stretching vibrations involving the octahedral units appear at much lower wavenumbers than those involving SiO_4 tetrahedral units. The infrared band at 765 cm^{-1} can be assigned primarily to a coupled Si–O stretching and P–O stretching vibration.

The lower wavenumber bands arise

TABLE II

OBSERVED AND CALCULATED WAVENUMBER (cm^{-1}) FOR CUBIC SiP_2O_7

Symmetry species	Wavenumber		Major contributors
	Observed	Calculated	
A_g (Raman)	1234	1252.5	f_{ra}, f_{rb}, f_{rc}
	1107	1095.3	f_{ra}, f_{rb},
	462	479.0	f_{ra}, f_{rb}, f_{ab} f_{ac}, f_{ad}, f_{ae} f_{af}
	353	365.8	f_{ra}, f_{aa}, f_{ab} f_{ac}, f_{ad}, f_{ae} f_{af}
E_g (Raman)	1192	1210.3	f_{rb}, f_{rc}
		715.8	f_{ra}, f_{rb}, f_{ac} f_{ad}
	589	596.7	f_{ra}, f_{rb}, f_{rc} f_{ac}, f_{ad}
	251.8	251.5	f_{ra}, f_{rb}, f_{rc} f_{aa}, f_{ab}, f_{ac} f_{ad}, f_{ae}, f_{af}
F_g (Raman)	1212	1216.9	f_{rb}, f_{rc}
	1143	1125.1	f_{ra}, f_{rb}
		794.7	f_{ra}, f_{rb}, f_{aa} f_{ac}
	564	576.9	f_{ra}, f_{rb}, f_{rc} f_{ac}, f_{ad}, f_{ae} f_{af}
	438	451.2	f_{ra}, f_{rb}, f_{ab} f_{ac}, f_{ad}
	429.2	442.1	f_{ra}, f_{rb}, f_{ab} f_{ac}, f_{ad}, f_{af}
	396	403.2	f_{ra}, f_{rb}, f_{ab} f_{ac}, f_{ad}, f_{af}
		336.0	f_{ra}, f_{rb}, f_{ab} f_{ac}, f_{ad}, f_{ae} f_{af}
	318	328.0	f_{rb}, f_{aa}, f_{ab} f_{ac}, f_{ad}, f_{ae} f_{af}
	283.6	299.7	f_{ra}, f_{rb}, f_{aa} f_{ab}, f_{ac}, f_{ad} f_{ae}, f_{af}
	235.0	231.4	f_{ra}, f_{rb}, f_{rc} f_{aa}, f_{ab}, f_{ac} f_{ad}, f_{ae}, f_{af}
	189.2	193.0	f_{ra}, f_{rb}, f_{rc} f_{aa}, f_{ab}, f_{ac} f_{ad}, f_{ae}, f_{af}

TABLE II—*Continued*

Symmetry species	Wavenumber		Major contributors
	Observed	Calculated	
F_u (infrared)	1230	1227.6	f_{rb}, f_{rc}
	1195	1215.8	f_{rc}
	1100	1089.7	f_{rb}, f_{ra}
	1052	1051.9	f_{rb}, f_{ra}
	1015	1034.1	f_{rc}, f_{ra}
	798	803.8	f_{ra}, f_{aa}, f_{ab}
	765	763.4	f_{ra}, f_{rb}, f_{rc} f_{aa}, f_{ac}
	732	739.9	f_{ra}, f_{rb}, f_{ac} f_{ad}
	675	678.5	f_{rb}, f_{rc}, f_{ac} f_{ad}
	639	623.2	f_{ra}, f_{rb}, f_{rc} f_{ac}, f_{ad}
	595	604.0	f_{ra}, f_{rb}, f_{rc} f_{ac}, f_{ad}
	510	514.7	f_{ra}, f_{rb}, f_{rc} f_{ac}, f_{ad}, f_{af}
	473	488.4	f_{ra}, f_{rb}, f_{rc} f_{ab}, f_{ac}, f_{ad} f_{af}
	212.7	221.6	f_{ra}, f_{rb}, f_{aa} f_{ab}, f_{ac}, f_{ad} f_{ae}, f_{af}
	183.9	184.0	f_{ra}, f_{rb}, f_{rc} f_{aa}, f_{ab}, f_{ac} f_{ad}, f_{ae}, f_{af}
	176.6	174.4	f_{ra}, f_{rb}, f_{aa} f_{ab}, f_{ac}, f_{ad} f_{ae}, f_{af}
	150.0	147.7	f_{ra}, f_{aa}, f_{ab} f_{ac}, f_{ad}, f_{ae} f_{af}

Note. Average error = 11.26 cm^{-1} or 2.116%.

from the coupling of a number of vibrational motions. The infrared band at 675 cm^{-1} is assigned primarily to a P–O stretching vibration involving a coupling of the motions of $P–O_I$ and $P–O_{II}$ stretching coordinates. The weak band at 639 cm^{-1} can be assigned to a delocalized vibration involving the Si–O, $P–O_I$, and $P–O_{II}$ stretching coordinates and the $O_I–P–O_I$ bending coordinates. It is interesting to note that vitreous SiP_2O_7 which contains SiO_4 units instead of SiO_6 units does not possess a band

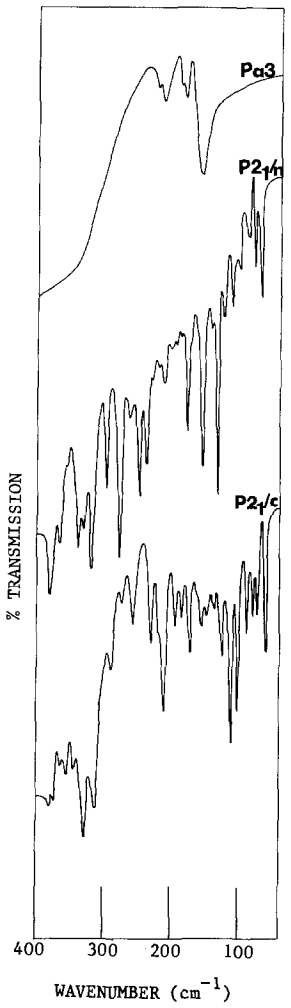

FIG. 4. The far-infrared spectra of various SiP_2O_7 polymorphs.

in this region (*12*). The weak shoulder at 595 cm^{-1} and strong band at 510 cm^{-1} in the infrared spectrum are assigned primarily to coupled Si–O and P–O_I stretching vibrations. The medium intensity band at 473 cm^{-1} is assigned to a delocalized vibration of mainly Si–O stretching and P–O_{II}–P and O_I–P–O_I bending coordinates. The bands observed in the far-infrared spectrum are primarily due to delocalized bending vibrations of different units. Their normal coordinate nature is indicated in Table II. The low wavenumber bands in the Raman spectrum also involve delocalized vibrations. For instance, the band at 564 cm^{-1} (F_g-species) arises primarily from the coupling of Si–O and P–O_I stretching vibrations. The most intense Raman band occurs at 353 cm^{-1} and is assigned to the A_g species on the basis of the NCA calculations. One would expect the most intense first-order mode to belong to the A_g species. The coordinate contributions to the various low wavenumber bands in the Raman spectrum are indicated in Table II. The refined set of calculated force constants for cubic SiP_2O_7 that generates these band assignments is listed in Table III.

C. Structural Considerations for Monoclinic SiP_2O_7

The unit cell of monoclinic SiP_2O_7 with space group C_{2h}^5 ($P2_1/c$) consists of four formula units per unit cell (*5*). This Bravais unit cell possesses four distorted SiO_6 octahedral and eight distorted PO_4 tetrahedral units. The Si–O bond lengths for the octahedral units range from 1.732 to 1.792 Å. The P–O bond lengths in the PO_4 tetrahedral units range from 1.493 to 1.581 Å. The interconnection of PO_4 tetrahedral and SiO_6 octahedral units in the monoclinic polymorph is similar to that of the cubic form.

Only stretching and bending coordinates have been considered for the normal coordinate analysis of this structure. Sixty-eight atoms were needed to define all 180 internal coordinates which define the system on the basis of the factor group and the selection rules. Again, the BvK correction was incorporated into the *G*-matrix calculation to consider the translationally equivalent atoms. The internal and symmetry coordinates for monoclinic SiP_2O_7 are listed elsewhere (*10*). Factor group analysis predicts the following selection rules for monoclinic SiP_2O_7:

$$\underset{(R)}{30A_g} + \underset{(R)}{30B_g} + \underset{(IR)}{29A_u} + \underset{(IR)}{28B_u}.$$

TABLE III

REFINED SET OF FORCE CONSTANTS FOR CUBIC AND MONOCLINIC SiP_2O_7 CRYSTALS

Cubic		Monoclinic	
Coordinate or interaction	Value	Coordinate or interaction	Value
Si–O (f_{ra})	3.4586	Si–O (short bond) (f_{ra})	3.5037
P–O_I (f_{rb})	5.5788	Si–O (long bond) (f_{rb})	3.1931
P–O_{II} (f_{rc})	5.3560	P–O (short bond) (f_{rc})	5.6579
O–Si–O (small angle) (f_{aa})	0.6451	P–O (long bond) (f_{rd})	5.6280
O–Si–O (large angle) (f_{ab})	0.5137	O–Si–O (average) (f_{aa})	0.6448
O–P–O (large angle) (f_{ac})	0.8323	O–P–O (large angle) (f_{ab})	0.9016
O–P–O (small angle) (f_{ad})	0.7239	O–P–O (small angle) (f_{ac})	0.8299
Si–O–P (f_{ae})	0.1612	Si–O–P (f_{ad})	0.2388
P–O–P (f_{af})	0.2290	P–O–P (f_{ae})	0.2595
(Si–O) (Si–O) (f_{rara})	0.1677	(Si–O) (Si–O) (average)(f_{rara})	0.1317
(Si–O) (O–Si–O large angle) (f_{raaa})	0.1555	(P–O) (O–P–O) (average) (f_{rcac})	0.1794
(Si–O) (O–Si–O small angle) (f_{raab})	0.1801	(Si–O) (O–Si–O) (average) (f_{raaa})	0.2508
(P–O) (P–O) (average) (f_{rbrb})	0.2926	(P–O) (O–P–O) (average) (f_{rcrc})	0.3723
(P–O) (O–P–O) (average) (f_{rbac})	0.1820		

Note. Units: stretch, mdyn/Å; bend, mdyn Å/rad^2; stretch/bend, mdyn/rad.

Due to the presence of a center of symmetry in the Bravais unit cell, no Raman-active band is active in the infrared spectrum and vice versa. The A_g- and B_g-species are Raman active, while the A_u- and B_u-species are infrared active. According to selection rules, 60 bands are active in the Raman spectrum, and 57 bands are active in the infrared spectrum.

The modified valence force field matrix used in this calculation consists of four stretching and five bending force constants, along with four interaction terms. The Si–O stretching coordinates are grouped into

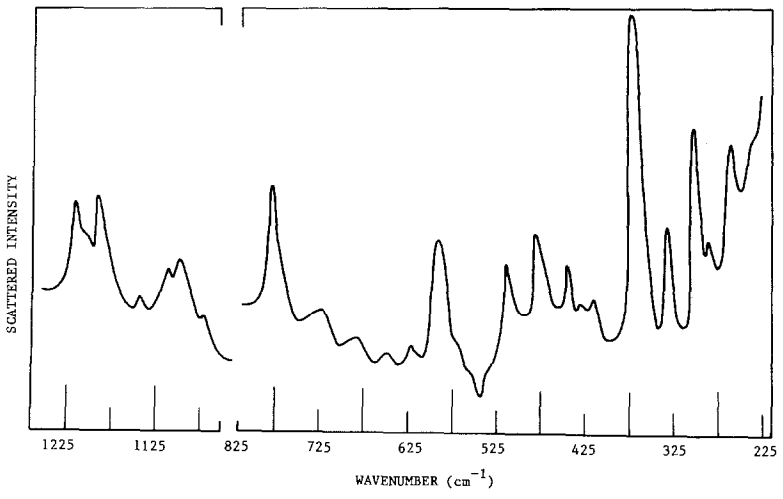

FIG. 5. The Raman spectrum of monoclinic ($P2_1/c$) SiP_2O_7.

two different classes depending on their bond lengths in order to simplify the force field. Si–O bond lengths ranging from 1.732 to 1.746 Å are grouped together, and their force constant is defined as f_{ra}. The force constant f_{rb} is associated with the stretching of Si–O bonds with length ranging from 1.766 to 1.792 Å. Similar considerations are made for defining the bending force constants. This procedure reduces the number of scalars (force constants) in the secular equation, and yields a reasonable set of calculated wavenumbers and force constants.

D. Vibrational Spectral Analysis for Monoclinic SiP_2O_7

The infrared and Raman spectra of monoclinic SiP_2O_7 are illustrated in Figs. 2 and 5, respectively. The observed and calculated wavenumbers are listed in Table IV. According to factor group analysis, 60 and 57 bands should be active in the Raman and infrared spectra, respectively. However, due to overlapping of bands and weak intensities for some bands, only 25 bands are observed in the Raman spectrum, and

TABLE IV

OBSERVED AND CALCULATED WAVENUMBERS (cm^{-1}) FOR MONOCLINIC SiP_2O_7

Symmetry species	Wavenumber		Wavenumber	
	Observed	Calculated	Observed	Calculated
A_g (Raman)	1217	1205.5	1205	1199.6
	1186	1166.2	—	1122.7
	—	1112.8	—	837.0
	—	806.0	—	792.4
	781	781.9	728	725.1
	680	683.7	504	538.2
	484	480.9	—	450.6
	—	427.0	415	411.5
	—	402.9	350	349.1
	—	334.2	—	330.5
	—	307.5	—	253.6
	255	249.9	—	166.0
	—	164.9	—	134.2
	—	103.1	—	95.6
	—	83.3	—	69.0
B_g (Raman)	1211	1200.0	—	1187.9
	—	1178.9	—	1160.2
	1135	1138.4	—	1112.7
	1115	1110.1	1065	1061.5
	1097	1054.3	—	1011.4
	—	814.6	—	804.3
	773	778.3	—	716.9
	—	648.9	—	586.2
	583	584.8	—	564.6
	472	471.9	456	455.9
	—	409.6	362	357.8
	326	317.4	—	298.8
	305	293.4	—	284.6
	—	269.3	279	280.1
	243	244.5	—	159.2

TABLE IV—*Continued*

Symmetry species	Wavenumber		Wavenumber	
	Observed	Calculated	Observed	Calculated
A_u (infrared)	1200	1199.3	—	1174.1
	1185	1163.8	—	1120.2
	1100	1105.6	—	795.2
	740	733.3	705	708.6
	678	691.1	600	590.1
	460	466.1	445	439.6
	443	431.6	390	387.6
	384	377.9	349.2	345.5
	331	329.0	293	287.7
	278.6	276.0	—	258.0
	212	203.3	184.7	194.8
	174.1	167.2	154.4	152.7
	—	127.1	111	113.2
	—	101.1	89.9	83.8
	74.7	72.4		
B_u (infrared)	—	1184.0	—	1157.5
	1140	1140.0	1060	1028.3
	1028	1025.4	—	1016.4
	—	989.6	—	790.5
	665	671.1	—	582.0
	572	577.4	515	543.5
	490	486.0	425	431.0
	—	423.6	378	371.6
	367	363.8	—	356.5
	358	353.3	316	315.4
	258	253.1	223.9	224.1
	193.8	199.4	—	185.7
	147.8	149.3	134.7	137.1
	124	125.1	80.2	81.0

Note. Average error = 13.87 cm^{-1} or 2.834%.

42 bands appear in the infrared spectrum. The assignment of all individual bands will not be discussed here in detail. Only the assignment of significant major bands to specific modes of vibration will be discussed in detail. The assignment of all observed vibrational bands for monoclinic SiP_2O_7 are consistent with those for cubic SiP_2O_7.

The strong infrared band at 1200 cm^{-1} is assigned to a P–O stretching vibration with A_u-symmetry. The corresponding Raman bands appear at 1217 and 1211 cm^{-1} with A_g- and B_g-symmetry, respectivly. The strong infrared bands at 1140 (B_u-species), 1060 (B_u-species), and 1100 cm^{-1} (A_u-species) are also assigned to stretching vibrations of P–O bonds. The correponding Raman bands appear at 1135 (B_g-species), 1115 (B_g-species), and 1186 cm^{-1} (A_g-species). The Raman bands at 1095 and 1065 cm^{-1} can be assigned mainly to coupled P–O stretching vibrations. The Raman band at 781 cm^{-1} is assigned to a coupled vibration with A_g-symmetry involving P–O stretching motions of PO_4 units and Si–O stretch-

ing motions of SiO_6 octahedral units. The infrared bands in the 790- to 700-cm^{-1} range are also assigned to similarly coupled modes of vibration. The bands below 550 cm^{-1} in both the infrared and Raman spectra are assigned primarily to the bending of O–Si–O, O–P–O, and Si–O–P bond angles. The strongest Raman band at 362 cm^{-1} is assigned to a combination of O–Si–O and O–P–O bending motions with A_g-symmetry. The strong infrared band at 515 cm^{-1} can be assigned to a delocalized mode involving O–P–O bending motion with B_u-symmetry. The complete potential energy distribution for this monoclinic SiP_2O_7 phase is reported elsewhere (*10*). The refined set of force constants for monoclinic SiP_2O_7 is listed in Table III. Their values are comparable with those for the cubic phase.

E. Interpretation of Trends in Force Constants

The calculated force constants for the Si–O stretching coordinates for SiO_6 octahedral units in cubic and monoclinic SiP_2O_7 occur in the 3.1–3.6 mdyn/Å range. As expected, this range is lower than the range for the Si–O stretching force constants of SiO_4 tetrahedral units (*8, 13*). This difference occurs because the A–O bonds in AO_6 units should be weaker than those in AO_4 units. However, the force constant for the Si–O stretching coordinates of stishovite (*10*), which also possesses SiO_6 units, is lower than those for the SiP_2O_7 polymorphs. One can account for this latter difference by the fact that each oxygen atom in stishovite is coordinated by three silicon atoms (*14*), while each oxygen atom in the SiP_2O_7 polymorphs coordinates to only two atoms. This structural difference should have a substantial effect on the magnitude of the Si–O stretching force constants.

The P–O stretching force constants for P_2O_7 groups in SiP_2O_7 crystals were found in the range of 5.3–5.7 mdyn/Å depending on the length of the P–O bond. As expected, the force constant decreased with the increase in bond length for each investigated phase. The values of P–O stretching force constants have been reported in the literature for NCA treatments using a model with isolated P_2O_7 ions for M(IV)P_2O_7-type materials (*15, 16*). The values of the P–O stretching and bending force constants obtained in this study agree well with the values reported by Hezel and Ross (*15*). The values reported by Mooney and Goldsmith (*16*) are higher than the calculated values in the present work. However, no consideration was made in either earlier study concerning the effect of the crystalline matrix on the vibrational modes of the P_2O_7 ion. This matrix effect can alter the force constants considerably. The factor group effect will also split the bands observed for isolated P_2O_7 ions. Thus, the symmetry associated with different vibrations of isolated P_2O_7 ions cannot be compared directly with those observed for SiP_2O_7 polymorphs. However, as predicted by both workers (*15, 16*), many of the P–O stretching vibrations occur in the 900- to 1200-cm^{-1} range. Similar predictions were made in this study regarding the P–O stretching vibrations of cubic and monoclinic SiP_2O_7 crystals. Also, the O–P–O bending vibrations for free P_2O_7 ions appear in the 400- to 750-cm^{-1} region. The NCA results obtained for cubic and monoclinic SiP_2O_7 crystals are consistent with those for free P_2O_7 ions. The bands noted in the above-mentioned range for SiP_2O_7 are associated with such bending vibrations along with minor contributions from other stretching and bending vibrations in the crystal structure.

The assignments made for cubic and monoclinic SiP_2O_7 have been valuable for predicting the structure of SiP_2O_7 glass (*12*). Comparison of vibrational spectra suggests that the glass material possesses SiO_4 units rather than SiO_6 units.

Conclusion

Normal coordinate analyses of the vibrational spectra for cubic ($Pa3$) and monoclinic ($P2_1/c$) SiP_2O_7 account for all first-order vibrational bands. Vibrations involving mainly Si–O stretching motions for SiP_2O_7 crystals with sixfold coordinated silicon atoms appear at lower wavenumbers than those for crystals with four-coordinated silicon atoms. As expected, the Si–O stretching force constants for the SiO_6 octahedral units (3.1–3.5 mdyn/Å) are much lower than those for SiO_4 tetrahedral units. The stretching force constants associated with P–O bonds are in the 5.3- to 5.7-mdyn/Å range. These values are comparable with those observed for other related pyrophosphate compounds (*15*, *16*).

References

1. V. F. Liebau, G. Bissert, and N. Koppen, *Z. Anorg. Allg. Chem.* **359,** 113 (1968).
2. V. H. Makart, *Helv. Chim. Acta* **50,** 399 (1967).
3. Joint Committee on Powder Diffraction Standards, Powder Diffraction Data for Cubic SiP_2O_7, 22-1321, Swarthmore, PA, International Center for Diffraction Data (1972).
4. C. M. Clark, D. K. Smith, and G. G. Johnson, Jr., "A FORTRAN IV Program for Calculating X-Ray Powder Diffraction Patterns, Version 7," Dept. of Geosciences, Pennsylvania State University, University Park, PA (1978).
5. V. G. Bisert and F. Liebau, *Acta Crystallogr. Sect. B* **26,** 233 (1970).
6. M. Born and K. Huang, "Dynamical Theory of Crystal Lattices," pp. 38–128, Oxford Univ. Press, London (1954).
7. G. Turrell, "Infrared and Raman Spectra of Crystals," pp. 178–193, Academic Press, New York (1972).
8. S. C. Cherukuri, Ph.D. thesis, Alfred University, Alfred, NY (1983).
9. G. R. Levi an G. Peyronel, *J. Kristallogr.* **92,** 190 (1935).
10. I. N. Chakraborty, Ph.D. thesis, Alfred University, Alfred, NY (1984).
11. C. K. Johnson, ORNL-3794, Oak Ridge National Laboratory, Oak Ridge, TN (1972).
12. I. N. Chakraborty and R. A. Condrate, Sr., *Phys. Chem. Glasses* **26,** 68 (1985).
13. I. Joseph, Ph.D. thesis, Alfred University, Alfred, NY (1985).
14. R. J. Hill, M. D. Newton, and G. V. Gibbs, *J. Solid State Chem.* **47,** 185 (1983).
15. A. Hezel and S. D. Ross, *Spectrochim. Acta Part A* **23,** 1583 (1967).
16. R. W. Mooney and R. L. Goldsmith, *J. Inorg. Nucl. Chem.* **31,** 937 (1969).